Preparation, Characterization, and Oxygen Barrier Properties of Regenerated Cellulose/Polyvinyl Alcohol Blend Films

Qianqian Zhu,[a,b] Jingjing Wang,[a] Jianzhong Sun,[a,*] and Qianqian Wang [a,c,d,e,f,*]

The application of cellulose materials for packaging usage has attracted a large amount of attention in recent years. In this study, cellulose was dissolved in a cold NaOH/urea solution. Transparent, strong, and flexible regenerated cellulose/polyvinyl alcohol (PVOH) films were fabricated *via* a solution blending and casting process. The physicochemical properties of the neat RC films, PVOH films, and RC-PVOH blend films were characterized *via* scanning electron microscopy, Fourier transform infrared spectroscopy, X-ray diffraction, thermogravimetric analysis, tensile tests, gas permeability, and ultraviolet-visible spectroscopy. The results of the physicochemical characterizations indicated that the RC-PVOH composite films with various PVOH contents yielded strong properties in terms of optical transparency, thermal stability, mechanical strength, and oxygen barrier performance. The RC-PVOH films with 8% PVOH loading exhibited a peak degradation temperature of 362 °C, a tensile strength of 80.8 MPa ± 0.3 MPa, and an oxygen permeability of 2.40 cm^3 x μm/m^2 x 24 h x kPa. The RC-PVOH composite films could be a competitive alternative as a packaging material to replace petroleum-based plastics.

Keywords: Cellulose solution; Blend casting; Mechanical property; Oxygen permeability

Contact information: a: Biofuels Institute, School of the Environment and Safety Engineering, Jiangsu University, Zhenjiang 212013 China; b: Analysis and Testing Center, Jiangsu University, Zhenjiang, 212013 PR China; c: Hunan Province Key Laboratory of Engineering Rheology, Central South University of Forestry and Technology, Changsha 410004 China; d: Institute of Chemical Industry of Forest Products, Chinese Academy of Forestry; Key Laboratory of Biomass Energy and Material, Jiangsu Province, Nanjing 210042, China; e: State Key Laboratory of Pulp and Paper Engineering, South China University of Technology, Guangzhou 510640 China; f: State Key Laboratory of Bio-Fibers and Eco-Textiles, Qingdao University, Qingdao 266071 China;
* Corresponding authors: Email: jzsun1002@ujs.edu.cn (SJZ); qianqian.wz@gmail.com (WQQ)

INTRODUCTION

Packing materials can provide effective barriers to light and oxygen, as well as to other chemicals, biological, and mechanical damage (Hubbe *et al.* 2017; Wang *et al.* 2018a). Petroleum-based plastics and synthetic plastic materials are ideal packaging materials, as the primary desirable features of plastic materials are their low cost, lightweight nature, easy processability, high stability and flexibility, and excellent physicochemical properties. However, plastic packaging materials are mostly permeable to gases and vapors, and thus they fail to prevent oxidation damage, which limits their application when impermeable barrier protection is required. In addition, considering the massive amount of plastic pollution, there has been a major increase in the interest of biodegradable polymers, *e.g.*, cellulose, starch, chitosan, and polylactic acid (PLA).

bioresources.com

The development of environmentally friendly, renewable, and biodegradable cellulose-based packaging materials that also exhibit high transparency and excellent barrier properties has exponentially expanded, but there are still many challenges (Wang *et al.* 2018a). Cellulose-based packaging materials, *e.g.*, regenerated cellulose films, surface-functionalized cellulose coatings, and cellulose nanocomposites, have been extensively investigated in order to improve the barrier strength and mechanical properties of paper and paperboard (Hubbe *et al.* 2017; Wang *et al.* 2018b; Zhu *et al.* 2020a,b). The application of thin coating layers of cellulose nanomaterials is a powerful tool for improving the mechanical and barrier properties of packaging materials. Spraying cellulose nanofibrils onto paper caused it to exhibit excellent oxygen barrier properties but increased its sensitivity to water vapor (Mirmehdi *et al.* 2018). As a low cost and non-toxic solvent, low-temperature NaOH/urea solution can dissolve cellulose with a high molecular weight (114,000 g/mole) rapidly (Wang *et al.* 2016). The cellulose solutions can be kept stable for one week. The low-temperature NaOH/urea solvent is recognized as a milestone in the history of cellulose processing technology. Biodegradable cellulose copolymer films were prepared by the NaOH/urea method followed by coating with chitosan and PVOH solution. The prepared biocomposites exhibited good physical properties as potential packaging materials. The composition-process-structure-property relationship of the resulting biocomposites was systematically investigated (Cazón, *et al.* 2018a,b, 2019). Optical transparent regenerated cellulose films that had a high oxygen permeability (0.003 cm^3 x μm/m^2 x 24 h x kPa to 0.03 cm^3 x μm/m^2 x 24 h x kPa) at 0% relative humidity (RH) were prepared from NaOH/urea solutions (Yang *et al.* 2011a). To improve the moisture barrier properties of cellulose films, multiple studies have incorporated other polymers or fillers into the films (Wu *et al.* 2012; Wang *et al.* 2018a). As such, the mechanical and water barrier properties of the altered cellulose films have been substantially improved without undermining their original valuable properties (Wang *et al.* 2018a).

As a promising packaging material, PVOH is water-soluble, has high film-forming ability, is biodegradable, and is biocompatible, but has a relatively low mechanical strength and high water uptake capacity (Dalei *et al.* 2019). Thus, PVOH packaging materials may be applicable for usage as packaging for hot food products that require high water vapor permeability (Jain *et al.* 2018). Cellulose/PVOH based biocomposites have recently been fabricated *via* different strategies (Abdulkhani *et al.* 2013; Cazón *et al.* 2018a,b 2019). Homogeneous dispersion of cellulose and plastic polymer is a huge challenge. Solution blending is widely used to achieve a good dispersion. To our best knowledge, there has been a lack of research concerning RC-PVOH composite films prepared by solution blending and casting. One such method, crosslinking, occurs when various crosslinking agents are introduced into the cellulose/PVOH composites.

Cellulose and PVOH, with their crystalline or semi-crystalline structures, could be interlinked *via* the hydrogen bonds between the hydroxyl groups. To take advantage of the properties of both cellulose and PVOH, various ratios of cellulose and PVOH solutions were blended together in aqueous form. The main goal of this study was to evaluate regenerated cellulose (RC) and PVOH composites films prepared *via* solution casting for their potential application as a packaging material. First, the cellulose was dissolved in a cold NaOH/urea (aq) solution, and the PVOH was dissolved in hot water. A series of RC-PVOH composite films were produced by changing the ratios of the blending solutions of cellulose and PVOH. Flexible, transparent, and oxygen

impermeable cellulose-based composite films were fabricated and characterized in the present study.

EXPERIMENTAL

Materials and Chemicals

Cotton linters with a viscosity average molecular weight of 1.07×10^5 kg mol^{-1} were obtained from Hubei Chemical Fiber Group Co., Ltd. (Xiangfan, China) and milled in a laboratory grinder to pass through a 40-mesh sieve. The flour obtained was oven-dried and used in the subsequent experiments. The polyvinyl alcohol 124 (PVOH-124, DP 2400), sodium hydroxide, urea, and concentrated sulfuric acid were all purchased from Sinopharm Chemical Reagent Co., Ltd. (Shanghai, China) and used as received.

Preparation of the RC Films and RC-PVOH Blend Films

A 4% cellulose solution was prepared by dissolving 4 g of cellulose flour in 96 g of a precooled NaOH and urea solution (in a ratio of 7 parts NaOH to 12 parts urea to 81 parts deionized water, by wt%) at -12 °C. The suspension was vigorously mixed for 5 min until a transparent solution was obtained. The air bubbles and small undissolved cellulose aggregates were then removed *via* centrifugation (Avanti-JE, Beckman Coulter, Brea, CA) at 8000 rpm for 10 min. A 4% PVOH solution was prepared by dissolving 4 g of PVOH in 96 g of deionized water at 90 °C for 2 h. The air bubbles were removed with an ultrasonic bath. The RC-PVOH composite films were produced by blending the cellulose and PVOH solutions at different ratios (100:0, 98:2, 95:5, 92:8, 90:10, and 0:100, which were labeled as RC, RC-PVOH2, RC-PVOH5, RC-PVOH8, RC-PVOH10, and PVOH, respectively). The resulting transparent solutions were degassed and cast on a glass plate and then coagulated in 1 L 5% H_2SO_4 bath for 5 min at room temperature. The obtained hydrogel films were washed with deionized water until a neutral pH was reached, and then they were dried on a stainless steel plate at room temperature.

Characterization

The surface and cross-section morphologies of the RC-PVOH films were observed *via* scanning electron microscopy (S-3400N, Hitachi, Tokyo, Japan). The specimens were sputter-coated with a thin layer of gold and then loaded in the S-3400N SEM at a low acceleration voltage (1 kV) for observation and photographing. The transmittance of the film was acquired from 200 nm to 800 nm using a DU-800 UV-Vis spectrophotometer (Beckman Coulter, Brea, CA), in triplicate. The final optical transmittance of the films was normalized with the thickness of the RC and RC-PVOH films of 0.036 mm. Fourier-transform infrared spectroscopy (FTIR) experiments were performed with a Nicolet Nexus 470 FTIR spectrometer (Thermo Nicolet Corporation, Waltham, MA) in a region range of 4000 cm^{-1} to 500 cm^{-1} with a resolution of 4 cm^{-1}. First, the composite films were ground into a fine powder in an agate mortar under a liquid nitrogen environment. The transparent pellets were then prepared by hydraulic pressing 2 mg of the sample mixture with 200 mg of KBr before FTIR viewing. Thermogravimetric analysis (TGA) of the films was performed with a Perkin Elmer TGA 4000 (PerkinElmer Inc., Waltham, MA) at a heating rate of 10 °C from 30 °C to 850 °C under nitrogen with a flow rate of 50 mL/min. Approximately 5 mg of the sample was used in each run. The X-ray diffraction (XRD) patterns of the composite films were recorded using a D8 Advance diffractometer (Bruker, Billerica, MA) from $2\theta = 5°$ to 2θ

= 35° at a scan speed of 2°/min at room temperature. The CuKα radiation source was operated at 30 kV and 15 mA. The tensile strength was determined *via* a tensile tester (Model YG026MB, Fangyuan Instrument Co. Ltd., Wenzhou, China) with a 1000 N load cell at a speed of 5 mm/min and at least 5 specimens were tested for each sample. The film oxygen permeability was measured using a VAC-V1 gas permeability tester (Labthink Instruments Co., Ltd., Boston, MA) according to standard GB/T1038 (2000). The oxygen permeability was determined at 23 °C, 0% RH, and with an area of 4.9 cm^2 in triplicate. The oxygen permeability was normalized with the thickness of the film, and the corresponding oxygen permeability was reported in cm^3 x μm/m^2 x 24 h x kPa.

RESULTS AND DISCUSSION

The images of the surface morphology of the blended films with various PVOH content are shown in Fig. 1a to Fig. 1e. As shown in the SEM images with different magnifications, *i.e.*, 370 x (Fig. 1e) to 3200 x (Fig. 1b to Fig. 1d), all the films exhibit relatively flat surfaces. Figure 1a' to Fig. 1e' show the cross-sections of the neat RC film and the RC-PVOH blend films. The microfibril structures of the RC films could be clearly seen in Fig. 1a'. Relatively smooth cross-sections with voids were observed in the RC-PVOH blend films, which was attributed to the incorporation of micro-scale PVOH fillers in the RC matrix. The SEM images of RC-PVOH2 and RC-PVOH5 reveal large cracks in the layered structures, whereas the image for the RC-PVOH8 film show relatively small and homogenously distributed voids. When the PVOH content increased to 10%, the layered structure with larger cracks was observed again in the RC-PVOH10 blend films. This phenomenon could be attributed to the phase separation of the PVOH in the RC matrix (Cano *et al.* 2015).
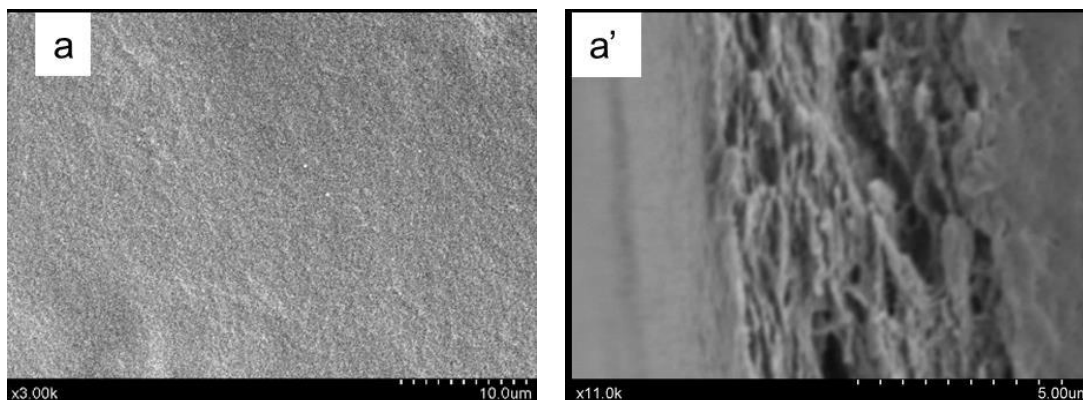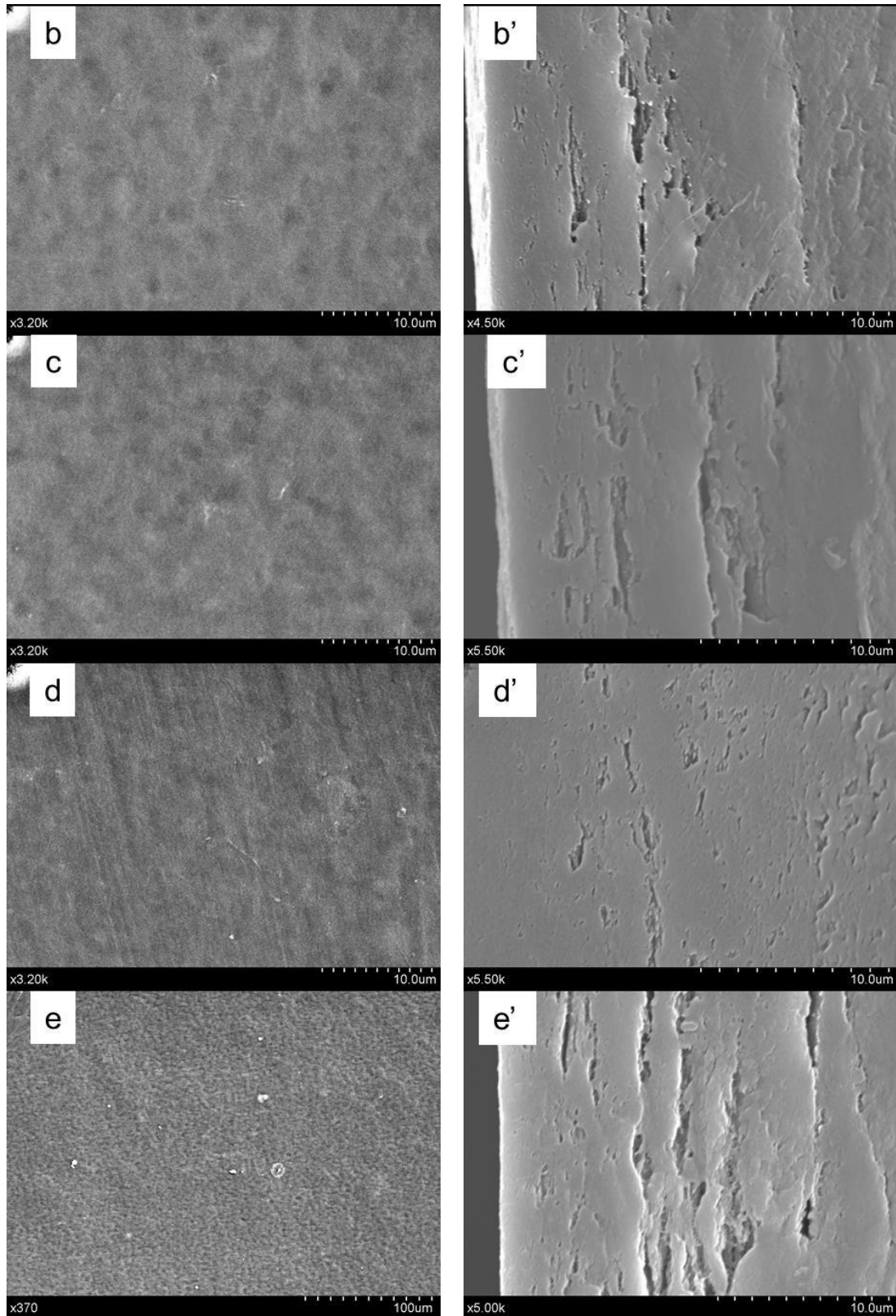
Fig. 1. SEM images of the surface and cross-sections of neat RC film and RC-PVOH blend films: (a, a') RC; (b, b') RC-PVOH2; (c, c') RC-PVOH5; (d, d') RC-PVOH8; and (e, e') RC-PVOH10

The adhesion that occurred between the RC and PVOH components enhanced the mechanical strength of the blend films. In summary, the concentration of PVOH could be an important parameter that affects the physio-chemical and structural properties of the RC-PVOH blend films.

The FTIR spectra of the neat RC film, PVOH film, and RC-PVOH composite films with various PVOH ratios are shown in Fig. 2a. The broad bands near 3430 cm^{-1} were assigned to the O-H stretching, whereas the bonds at approximately 2900 cm^{-1} were assigned to the C-H stretching in both the RC and PVOH films. The O-H band tends to form hydrogen bonding, which is likely to affect the mechanical properties of the films (Cazón *et al*. 2019). The band at 2900 cm^{-1} reflects the change in the cellulose crystal structure (Abdulkhani *et al*. 2013). The absorption bands at 1720 cm^{-1} assigned to the C=O bending vibration in the PVOH film were absent in the RC-PVOH blend films, which was likely due to overlapping signals from the nearby 1630 cm^{-1} C=O stretching peak. Other characteristic bands were observed at 1165 cm^{-1}, 1060 cm^{-1}, and 899 cm^{-1}. The band at 1165 cm^{-1} was assigned to the C-O-C vibration. The bands at 1060 cm^{-1} and 899 cm^{-1} were recognized as the C-O stretching and the C-H deformation, respectively (Wang *et al*. 2015).

As shown in Fig. 2a, the ratio of PVOH in the film had little effect on the overall infrared spectra of RC-PVOH composite films, since the FTIR spectra of the cellulose and PVOH composites had strong overlapping signals. Although the interfacial interactions between cellulose and PVOH are still not fully understood, the abundance of hydroxyl groups of RC and PVOH suggests a tendency to form intermolecular hydrogen bonding. FTIR results indicated that there are no other chemical interactions between the cellulose and PVOH molecules besides hydrogen bonding (Abdulkhani *et al*. 2013; Voronova *et al.* 2015; Salehpour *et al.* 2018).
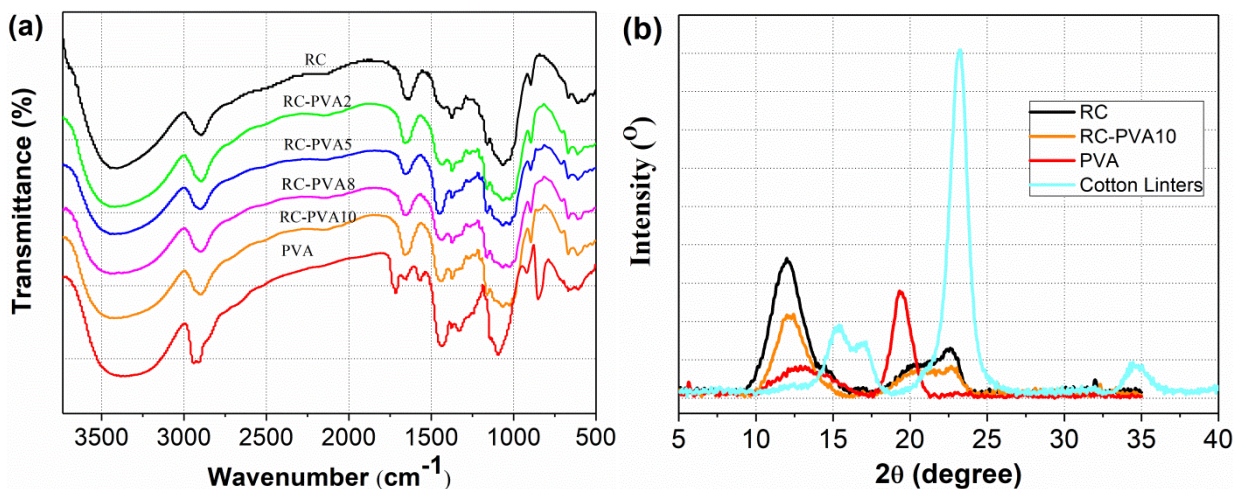

Fig. 2. The FTIR and XRD spectra: (a) the FTIR spectra of the RC film, RC-PVOH composite films, and PVOH film; (b) the X-ray diffractograms of the RC-PVOH10 film compared to the cotton linters, neat RC, and PVOH films

Figure 2b shows the XRD patterns of the neat RC film, PVOH film, and RC-PVOH blend films. The cotton linters had typical cellulose I diffraction peaks at $2\theta =$ 15.4°, $2\theta =$ 17.1°, and $2\theta =$ 23.2° for (1 $\bar{1}$ 0), (110), and (200), respectively. Peaks at $2\theta =$ 12.0°, $2\theta =$ 20.0°, and $2\theta =$ 22.6° were attributed to the (1 $\bar{1}$ 0), (110), and (020) plane for

cellulose II (Li *et al.* 2015; Qi *et al.* 2009). It was reported that cellulose I and II coexisted in the RC films regenerated from a NaOH/urea solution. It was noted that the ($1\bar{1}0$) plane was stronger than the (110) and (200) peaks for cellulose II. This unusual phenomenon had previously been reported by Li *et al.* (2015) and Qi *et al.* (2009). The neat PVOH films exhibited two peaks at $2\theta = 12.9°$ and $2\theta = 19.3°$.

It was reported that the increase in PVOH content would decrease the cellulose crystallinity significantly (Zhang *et al.* 2012). On the other hand, the increase in cellulose content could also undermine the crystallinity of PVOH as reported by Lam, *et al.* (2017). The RC-PVOH blend films displayed a mixed diffraction pattern of characteristics from cellulose I, cellulose II, and PVOH.
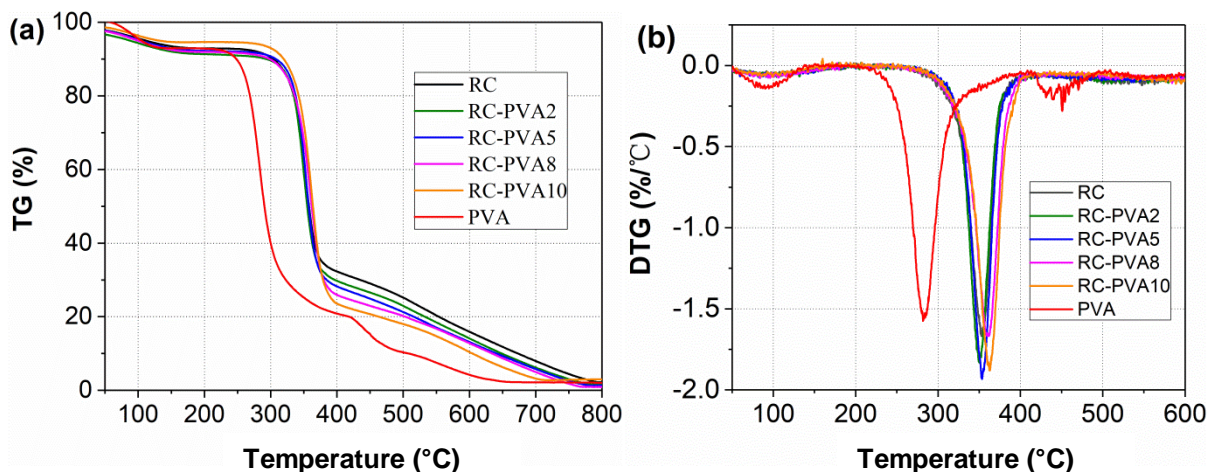

Fig. 3. The thermogravimetric analysis curves of the neat PVOH, RC, and RC-PVOH blend films: (a) TGA curve; (b) DTG curve

A high level of thermal stability is critical for packaging materials under harsh thermal environments. Thermogravimetric analysis and DTG were used to evaluate the thermal decomposition of the RC-PVOH composite films, as shown in Figs. 3a and 3b. The thermal degradation of neat PVOH occurred in two stages; the first stage occurred at approximately 250 °C to 350 °C (approximately 70% of the initial weight), and the second stage occurred at approximately 420 °C to 600 °C (approximately 20% of the initial weight). Similar results were reported by Yang *et al.* (2011b). The maximum decomposition temperature of the neat PVOH was 282 °C. A two-stage decomposition was also observed for RC film at approximately 300 °C to 380 °C and at approximately 400 °C to 700 °C, with a much higher peak temperature of 353 °C, as shown in the DTG curve. It could be observed in Fig. 3 that no noticeable differences in the TGA and DTG curve shapes for the neat RC and RC-PVOH blend films were detected at temperatures below 200 °C. There were some visible differences between the neat RC film and the RC-PVOH blend films when the temperature was higher than 400 °C. The RC-PVOH blend films with a higher ratio of PVOH to RC had a relatively low residual mass. The RC-PVOH composite films began to thermally decompose at temperatures greater than 300 °C (as shown in Fig. 3a). As the ratio of PVOH to RC increased in the composite films, so did the peak temperature of the derivative weight curve; the peak temperatures for RC-PVOH2, RC-PVOH5, RC-PVOH8, and RC-PVOH10 were 350 °C, 354 °C, 362 °C, and 363 °C, respectively (as shown in Fig. 3b). The thermal decomposition

process indicated that the thermal degradation temperatures of the RC-PVOH composite films were nearly identical to those of the neat RC film.

The tensile strength and oxygen permeability of the RC-PVOH films as functions of the ratio of PVOH to RC are shown in Figs. 4a and 4b, respectively. The neat RC film without PVOH had a tensile strength of 76.8 MPa ± 0.6 MPa. The structural defects, *i.e.*, cracks and voids, in the blend composite films were decreased because of the increased ratio of PVOH to RC. The tensile strength of the RC-PVOH composite films steadily increased from 77.1 MPa ± 1.1 MPa to 80.8 MPa ± 0.3 MPa as the PVOH content increased from 2% to 8%. The increased tensile strength could also be related to the newly formed hydrogen bonds between the cellulose and PVOH molecules (Kondo and Sawatari 1998). The RC-PVOH8 film had the highest tensile strength. However, the addition of more PVOH (10%) resulted in a noticeable reduction in tensile strength (79.9 MPa ± 0.7 MPa), which is likely due to the possible agglomeration and inhomogeneous dispersion, as indicated by the SEM images. The structure defects led to poor interface interaction between PVOH and RC (Quero *et al*. 2018).
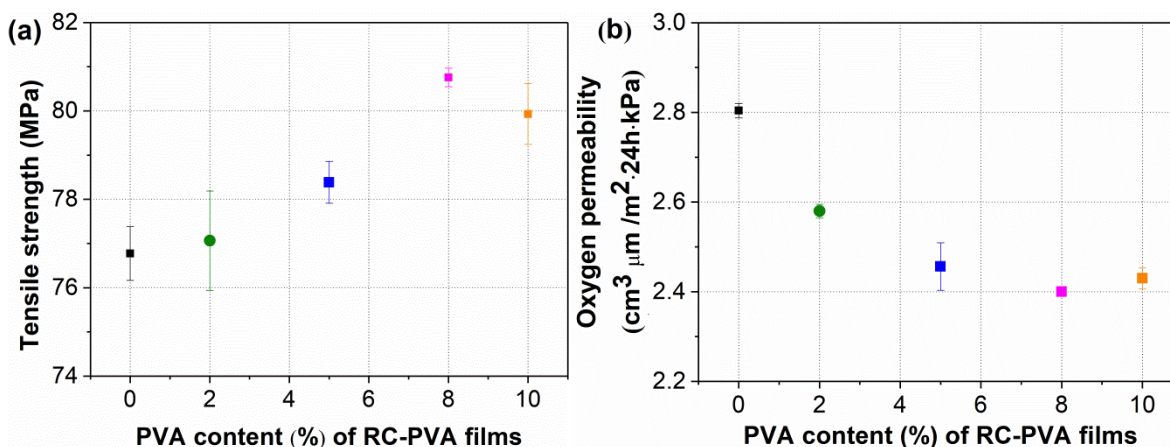

Fig. 4. The effect of the ratio of PVOH to RC on the tensile strength and oxygen permeability of RC-PVOH: (a) tensile strength; (b) oxygen permeability

Table 2. Oxygen Permeability of Cellulose or Starch Biocomposites

Sample	Composites preparation	Humidity	Oxygen permeability $cm^3 \cdot \mu m/m^2 \cdot 24h \cdot kPa$	Reference
RC-PVOH8	Solution blending and casting	0%	2.4	This study
PLA30C	melt-blending and hot press	65%	72	(Battegazzore *et al*. 2014)
PA 6.10_5C	melt-blending and hot press	50%	18	(Battegazzore *et al*. 2018)
Thermoplastic starch	melt-blending and hot press	25%	22	(Battegazzore *et al*. 2015)

Figure 4b shows the effect of the ratio of PVOH to RC on the oxygen permeability of the composite films. The oxygen permeability of the neat RC films at 0% RH was 2.80 cm^3 x μm/m^2 x 24 h x kPa, while the oxygen permeability of the RC-PVOH

bioresources.com

composite films with a ratio of PVOH to RC ranging from 2% to 10% at 0% RH steadily declined from 2.58 cm^3 x μm/m^2 x 24 h x kPa to 2.43 cm^3 x μm/m^2 x 24 h x kPa (as shown in Fig. 4b). The RC-PVOH8 film had an even lower value (2.40 cm^3 x μm/m^2 x 24 h x kPa), which was considered in the high range (40 cm^3 x μm/m^2 x 24h x atm to 400 cm^3 x μm/m^2 x 24h x atm) (Wang *et al.* 2018a).

The oxygen permeability of the RC-PVOH composite films at 0% RH was lower than the reported data by Syverud and Stenius (2008) for microfibrillated cellulose films (3.52 cm^3 x μm/m^2 x 24 h x kPa to 5.03 cm^3 x μm/m^2 x 24 h x kPa), slightly higher than that of neat PVOH films (2.06 cm^3 x μm/m^2 x 24 h x kPa) (Chen *et al.* 2017). The oxygen permeability of several biocomposites is listed in Table 2. However, it was difficult to compare their oxygen permeability due to the different raw materials used, the processing methodologies, and testing conditions adopted.
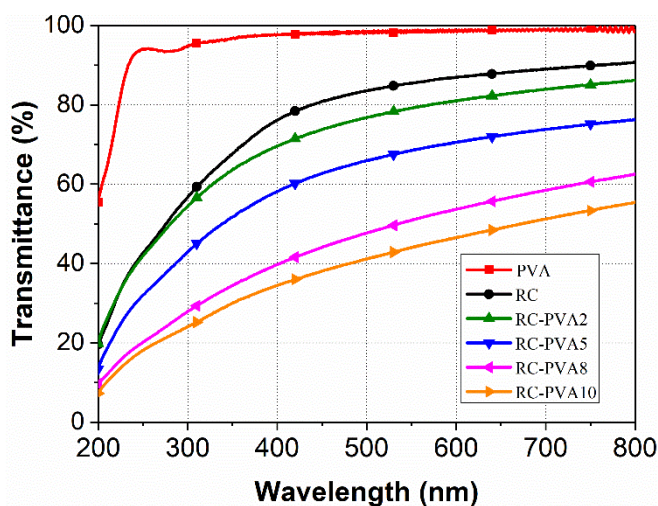

Fig. 5. The effect of the ratio of PVOH to RC on the transparency of the RC-PVOH films

Figure 5 displays the light transmittance of the pure PVOH film, RC film, and RC-PVOH films at a wavelength of 200 nm to 800 nm. The obtained neat PVOH films showed excellent optical transparency with a mean value greater than 95% at a wavelength of 300 nm to 800 nm. The transmittance value of the neat RC film was lower than the neat PVOH film. The ratio of PVOH to RC could be a vital factor in influencing the structure and transparency properties of the RC-PVOH blend films. Overall, the transmittance values of RC-PVOH blend films were much lower than the neat PVOH and RC films at the wavelength of 300 nm to 800 nm, which indicated that the blending of PVOH with RC undermined the transparency of the blend films. The transmittance values decreased with the increase in PVOH proportions. Similar results were reported by Yuwawech *et al.* (2015) and Salehpour *et al.* 2018. The RC-PVOH10 film showed the lowest visible light transmittance values, which was still greater than 40% at a range of 400 nm to 750 nm. This was probably due to the heterogeneous dispersion of PVOH and the formation of voids within the RC matrix, as revealed by the SEM. It was reported by Salehpour *et al.* (2018) that the surface roughness could also affect the light adsorption and transmittance values due to light scattering and the loss of the incident light intensity.

CONCLUSIONS

1. The RC-PVOH composite films with different ratios of PVOH to RC were synthesized *via* a process of solution blending and casting.

2. The PVOH content was an important factor affecting the structural properties of the RC-PVOH films, as indicated by the SEM and UV-Vis spectra. The interactions between the RC and PVOH molecules were primarily physical interactions instead of chemical interactions.

3. The RC-PVOH films exhibited high levels of thermal stability, tensile strength, and oxygen permeability. The RC-PVOH composite film with 8% PVOH displayed the best results, with a peak degradation temperature of 362 °C, a tensile strength of 80.8 MPa ± 0.3 MPa, and an oxygen permeability of 2.40 cm^3 x $\mu m/m^2$ x 24 h x kPa.

ACKNOWLEDGMENTS

REFERENCES CITED

Abdulkhani, A., Marvast, E. M., Ashori, A., Hamzeh, Y., and Karimi, A. N. (2013). "Preparation of cellulose/polyvinyl alcohol biocomposite films using 1-n-butyl-3-methylimidazolium chloride," *International Journal of Biological Macromolecules* 62, 379-386. DOI: 10.1016/j.ijbiomac.2013.08.050

Battegazzore, D., Bocchini, S., Alongi, J., Frache, A. and Marino, F. (2014). "Cellulose extracted from rice husk as filler for poly(lactic acid): Preparation and characterization," *Cellulose* 21(3), 1813-1821. DOI: 10.1007/s10570-014-0207-5

Battegazzore, D., Bocchini, S., Nicola, G., Martini, E., and Frache, A. (2015). "Isosorbide, a green plasticizer for thermoplastic starch that does not retrograde," *Carbohydrate Polymers* 119, 78-84. DOI: 10.1016/j.carbpol.2014.11.030

Battegazzore, D., Sattin, A., Maspoch, M.L., and Frache, A. (2018). "Mechanical and barrier properties enhancement in film extruded bio-polyamides with modified nanoclay," *Polymer Composite* 40(7), 2617-2628. DOI: 10.1002/pc.25056

Cano, A., Fortunati, E., Cháfer, M., González-Martinez, C., Chiralt, A., and Kenny, J. M. (2015). "Effect of cellulose nanocrystals on the properties of pea starch-poly(vinyl alcohol) blend films," *Journal of Material Science* 50(21), 6979-6992. DOI: 10.1007/s10853-015-9249-9

Cazón, P., Vázquez, M., and Velazquez, G. (2018a) "Composite films of regenerate cellulose with chitosan and polyvinyl alcohol: Evaluation of water adsorption, mechanical and optical properties," *International Journal of Biological Macromolecules* 117, 235-246. DOI: 10.1016/j.ijbiomac.2018.05.148

Cazón, P., Vázquez, M., and Velazquez, G. (2018b). "Novel composite films based on cellulose reinforced with chitosan and polyvinyl alcohol: Effect on mechanical properties and water vapour permeability," *Polymer Testing* 69, 536-544. DOI: 10.1016/j.polymertesting.2018.06.016

Cazón, P., Velazquez, G., and Vázquez, M. (2019). "Novel composite films from regenerated cellulose-glycerol-polyvinyl alcohol: Mechanical and barrier properties," *Food Hydrocolloid* 89, 481-491. DOI: 10.1016/j.foodhyd.2018.11.012

Chen, C., Chen, Y., Xie, J., Xu, Z., Tang, Z., Yang, F., and Fu, K. (2017). "Effects of montmorillonite on the properties of cross-linked poly(vinyl alcohol)/boric acid films," *Progress in Organic Coatings* 112, 66-74. DOI: 10.1016/j.porgcoat.2017.06.003

Dalei, G., Das, S., Jena, S. R., Nayak, J., Samanta, L., and Das, S. P. (2019). "Surface modification of cellulose/polyvinyl alcohol biocomposites by non-thermal argon plasma: Applications towards biological relevance," *Cellulose* 26(4), 2437-2451. DOI: 10.1007/s10570-019-02243-0

GB/T 1038-2000 (2000). "Plastics – Film and sheeting – Determination of gas transmission – Differential-pressure method," Standardization Administration of China, Beijing, China.

Hubbe, M. A., Ferrer, A., Tyagi, P., Yin, Y., Salas, C., Pal, L. and Rojas, O. J. (2017). "Nanocellulose in thin films, coatings, and plies for packaging applications: A review," *BioResources* 12(1), 2143-2233. DOI: 10.15376/biores.12.1.2143-2233

Jain, N., Singh, V. K., and Chauhan, S. (2018). "A review on mechanical and water absorption properties of polyvinyl alcohol based composites/films," *Journal of the Mechanical Behavior of Materials* 26(5-6), 213-222. DOI: 10.1515/jmbm-2017-0027

Kondo, T., and Sawatari C (1998). "Interchain hydrogen bonds in cellulose—poly(vinyl alcohol) characterized by differential scanning calorimetry and solid-state nmr analyses using cellulose model compounds," in: *Cellulose Derivatives: Modification, Characterization, and Nanostructures*, T. J. Hienze, and W. G. Glasser (ed.), American Chemical Society, Washington, D.C., pp. 296-305. DOI: 10.1021/bk-1998-0688.ch021

Lam, N. T., Chollakup, R., Smitthipong, W., Nimchua, T., and Sukyai, P. (2017). "Utilizing cellulose from sugarcane bagasse mixed with poly(vinyl alcohol) for tissue engineering scaffold fabrication," *Industrial Crops and Products* 100, 183-197. DOI: 10.1016/j.indcrop.2017.02.031

Li, R., Wang, S., Lu, A., and Zhang, L. (2015). "Dissolution of cellulose from different sources in an NaOH/urea aqueous system at low temperature," *Cellulose* 22(1), 339-349. DOI: 10.1007/s10570-014-0542-6

Mirmehdi, S., de Oliveira, M. L. C., Hein, P. R. G., Dias, M. V., Sarantópoulos, C. I. G. D., and Tonoli, G. H. D. (2018). "Spraying cellulose nanofibrils for improvement of tensile and barrier properties of writing & printing (W&P) paper," *Journal of Wood Chemistry Technology* 38(3), 233-245. DOI: 10.1080/02773813.2018.1432656

Qi, H., Cai, J., Zhang, L., and Kuga, S. (2009). "Properties of films composed of cellulose nanowhiskers and a cellulose matrix regenerated from alkali/urea solution," *Biomacromolecules* 10(6), 1597-1602. DOI: 10.1021/bm9001975

Quero, F., Padilla, C., Campos, V., Luengo, J., Caballero, L., Melo, F., Li, Q., Eichhorn, S. J., and Enrione, J. (2018). "Stress transfer and matrix-cohesive fracture mechanism in microfibrillated cellulose-gelatin nanocomposite films," *Carbohydrate Polymers* 195, 89-98. DOI: 10.1016/j.carbpol.2018.04.059

Salehpour, S., Rafieian, F., Jonoobi, M., and Oksman, K. (2018). "Effects of molding temperature, pressure and time on polyvinyl alcohol nanocomposites properties produced by freeze drying technique," *Industrial Crops and Products* 121, 1-9. DOI: 10.1016/j.indcrop.2018.04.079

Syverud, K., and Stenius, P. (2008). "Strength and barrier properties of MFC films," *Cellulose* 16(1), 75-85. DOI: 10.1007/s10570-008-9244-2

Voronova, M. I., Surov, O. V., Guseinov, S. S., Barannikov, V. P., and Zakharov, A. G. (2015). "Thermal stability of polyvinyl alcohol/nanocrystalline cellulose composites," *Carbohydrate Polymers* 130, 440-447. DOI: 10.1016/j.carbpol.2015.05.032

Wang, Q., Wei, W., Kingori, G. P., and Sun, J. (2015). "Cell wall disruption in low temperature NaOH/urea solution and its potential application in lignocellulose pretreatment," *Cellulose* 22(6), 3559-3568. DOI: 10.1007/s10570-015-0767-z

Wang, S., Lu, A., and Zhang, L. (2016). "Recent advances in regenerated cellulose materials," *Progress in Polymer Science* 53, 169-206. DOI: 10.1016/j.progpolymsci.2015.07.003

Wang, J., Gardner, D. J., Stark, N. M., Bousfield, D. W., Tajvidi, M., and Cai, Z. (2018a). "Moisture and oxygen barrier properties of cellulose nanomaterial-based films," *ACS Sustainable Chemistry & Engineering* 6(1), 49-70. DOI: 10.1021/acssuschemeng.7b03523

Wang, Q., Sun, J., Yao, Q., Ji, C., Liu, J., and Zhu Q. (2018b). "3D printing with cellulose materials," *Cellulose* 25(8), 4275-4301. DOI: 10.1007/s10570-018-1888-y

Wu, C.-N., Saito, T., Fujisawa, S., Fukuzumi, H., and Isogai, A. (2012). "Ultrastrong and high gas-barrier nanocellulose/clay layered composites," *Biomacromolecules* 16(3), 1927-1932. DOI: 10.1021/bm300465d

Yang, H., Xu, S., Jiang, L., and Dan, Y. (2011b). "Thermal decomposition behavior of poly (vinyl alcohol) with different hydroxyl content," *Journal of Macromolecular Science, Part B* 51(3), 464-480. DOI: 10.1080/00222348.2011.597687

Yang, Q., Fukuzumi, H., Saito, T., Isogai, A., and Zhang, L. (2011a). "Transparent cellulose films with high gas barrier properties fabricated from aqueous alkali/urea solutions," *Biomacromolecules* 12(7), 2766-2771. DOI: 10.1021/bm200766v

Yuwawech, K., Wootthikanokkhan, J., and Tanpichai, S. (2015). "Effects of two different cellulose nanofiber types on properties of poly(vinyl alcohol) composite films," *Journal of Nanomaterials* 2015, 1-10. DOI: 10.1155/2015/908689

Zhang, X., Zhu, J., and Liu, X. (2012). "Preparation and characterization of regenerated cellulose blend films containing high amount of poly(vinyl alcohol) (PVOH) in ionic liquid," *Macromolecular Research* 20(7), 703-708. DOI: 10.1007/s13233-012-0106-2

Zhu, Q., Liu, S., Sun, J., Liu, J., Kirubaharan, C.J., Chen, H., Xu, W., and Wang, Q. (2020a). "Stimuli-responsive cellulose nanomaterials for smart applications," *Carbohydrate Polymers* 235, 115933. DOI: 10.1016/j.carbpol.2020.115933

Zhu, Q., Yao, Q., Sun, J., Chen, H., Xu, W., Liu, J., and Wang, Q. (2020b). "Stimuli induced cellulose nanomaterials alignment and its emerging applications: A review," *Carbohydrate Polymers* 230, 115609. DOI: 10.1016/j.carbpol.2019.115609